Fatigue Strength Depending on Position of Cracks for Weldments

Hae Woo Lee*

Welding Research Team, Hanjin Heavy Industries,
Busan, Korea

Won Jo Park

School of Mechanical and Aerospace Engineering, Gyeongsang National University,
Institute of of Marine Industry, Kyeongnam, Korea

This is a study of fatigue strength of weld deposits with transverse cracks in plate up to 50 mm thick. It is concerned with the fatigue properties of welds already with transverse cracks. A previous study of transverse crack occurrence, location and microstructure in accordance with welding conditions was published in the Welding Journal (Lee et al., 1998). A fatigue crack develops as a result of stress concentration and extends with each load cycle until fatigue occurs, or until the cyclic loads are transferred to redundant members. The fatigue performance of a member is more dependent on the localized state of stress than the static strength of the base metal or the weld metal. Fatigue specimens were machined to have transverse cracks located on the surface and inside the specimen. Evaluation of fatigue strength depending on location of transverse cracks was then performed. When transverse cracks were propagated in a quarter- or half-circle shape, the specimen broke at low cycle in the presence of a surface crack. However, when the crack was inside the specimen, it propagated in a circular or elliptical shape and the specimen showed high fatigue strength, enough to reach the fatigue limit within tolerance of design stresses.

Key Words : Fatigue Strength, Transverse Cracks, Surface Crack, Inside Crack, Thick-Plate Weldments

1. Introduction

As welded structures become bigger, thick-plate welding becomes more important. Thick-plate weldments have higher cooling rates and greater restraint stresses than thin-plate weldments, making it easier for cracks to occur in the thick welded parts. This is the weakest area because its heating and cooling creates inconsistent microstructure. Safety is very important in this type of weld fabrication. Cracking is not allowed in the weldment, although in some cases certain porosity is allowed.

"Complete joint penetration groove welds in butt joints transverse to the direction of computed tensile stress shall have no visible piping porosity," according to AWS D1.1, Structural Welding Code-Steel (ANSI/AWS D1.1-98). "For all other groove welds and for fillet welds, the sum of the visual piping porosity 1 mm or greater in diameter shall not exceed 10 mm in any linear inch of weld and shall not exceed 19 mm in any 305 mm length of weld," the code continues. It is well known that porosity has a round edge while a crack is sharp, making it easy 'to propagate. Crack propagation is different depending on crack size and location. Fatigue in welded structures has been studied extensively, especially with recent developments in fracture mechanics. Research on

---

* Corresponding Author,
  E-mail : hw6308@hanmail.net
  TEL : +82-55-410-3375; **FAX** : +82-55-410-8481
  Welding Research Team, Hanjin Heavy Industries, Busan, Korea. (Manuscript **Received** December 22, 2005; **Revised** March 3, 2006)

fatigue crack propagation is also extensive (Tsay et al., 1999 ; Lu et al., 1993 ; Zhang et al., 1999). But in most studies of fatigue, experiments were performed by machined notch or artificially induced discontinuity. Up until now, few investigations of cracks occurring in the actual structure have been undertaken. In this study, therefore, specimens were fabricated and welded like the actual structure and machined to have transverse cracks on the surface and inside. Fatigue properties, depending on crack location, were then studied, as well as the distance between the transverse crack and porosity.

2. Experimental Procedure

2.1 Test panel

The size of the test panel was 2000 mm long × 1800 mm wide × 50 mm thick. The panel was fabricated from ABS EH32 TMCP, high-strength hull steel, to provide test conditions similar to actual construction conditions — Fig. 1. To magnify fabrication-related weld residual stresses, the welding jig and test panel were fillet-welded together.

2.2 Test weldments

Two sets of test panels were made of the same size and morphology as shown in Fig. 1, with specimen sections welded in layers, as shown in Fig. 2. To compare the residual stresses and position of occurrence of the transverse cracks, the sections were welded under the following conditions :

(1) One was welded with preheating and interpass temperatures below 30℃.
(2) The other was welded with preheating and interpass temperatures of 100-120℃.

The preheat temperature of 100℃ was obtained from the Yurioka chart method (Yurioka, 1995) (using Table 1, 50-mm-thick steel plate, Ceq 0.34). The test specimens were welded using 100-120℃ in consideration of ambient temperatures. The panel was welded with AWS A5.29 E81T1-K2 electrodes, using the flux cored arc welding processes (1.2 mm diameter, 20 L/mim flow rate,
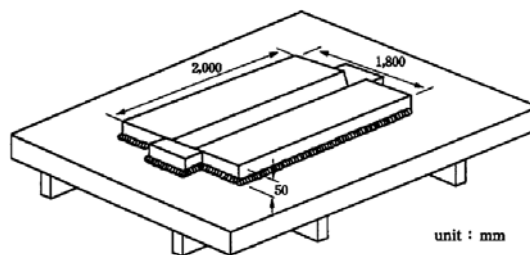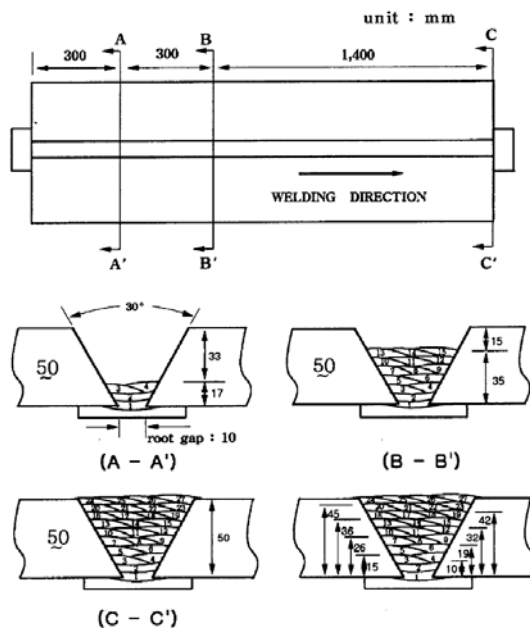

Fig. 1 Schematic of weld panel

Fig. 2 Schematic of weld deposit

100% CO_2 gas, semiautomatic, electrode extension 25-30 mm). Welding parameters are shown in Table 2.

### 2.3 Chemical composition/strength

A spectroanalyzer (Baird Spectrovac-2000, USA) was used to determine the chemical composition of the base and weld metal. Mean values of the three specimens were then recorded in Tables 1. Other test results such as hardness, microstructure, residual stresses, absorbed energy, diffusible hydrogen content and crack position were published in a previous study (Lee et al., 1998). Strength was measured using a universal testing machine (Shimadzu UH-F100A, Japan). Tensile test specimens were made from all deposited metal

Table 1 Chemical composition of Base/Weld Metal

%	C	Si	Mn	P	S	Ni	Ti	Ts (kgf/mm²)	Ys (kgf/mm²)	El (%)
EH32 TMCP	0.18 max.	0.10 ~0.50	0.90 ~1.60	0.040 max.	0.040 max.	0.40 max.	0.02 max.	45~60	32.0	20.0
Base Metal	0.09	0.38	1.35	0.015	0.005	0.03	0.02	52.8	38.0	31.0
Weld metal A	0.04	0.29	1.05	0.012	0.017	1.32	0.01	69.4	63.7	22.8
Weld metal B	0.04	0.29	1.03	0.013	0.016	1.31	0.01	66.3	61.4	23.4

Table 2 Welding Parameters

Identification	Welding Condition	Pass (No.)	Current (A)	Voltage (V)	Speed (Cm/min)	Heat input (KJ/cm)
A	Preheating/interpass temperature below 30℃	1	240~250	30	16	25
		2~27	340~350	35	37~41	26
B	Preheating/interpass temperature 100 ; 120℃	1	240~250	30	15	29
		2~27	340~350	35	38~42	25
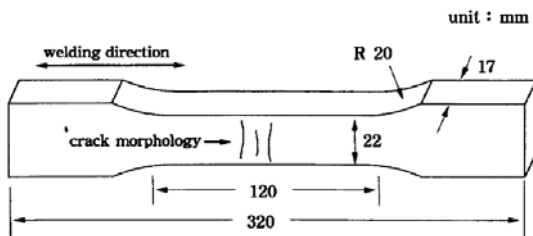
Fig. 3 Schematic of all-weld-metal fatigue test specimen

in a direction parallel to the welding direction. The specimens were the round-bar type, taken 10 mm from the weld face, and recorded in Tables 1.
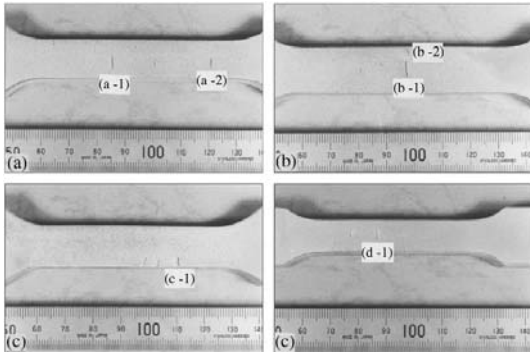
2.4 Fatigue test

Fatigue specimens were collected from samples welded with preheat and interpass temperatures below 30℃. Test equipment was a ±20-ton capacity, axial tension fatigue tester. Testing was performed by load control at a stress ratio=0.1 with sine wave and frequency of 3 Hz, at room temperature. Fatigue test specimens from deposit metal were made to have a tension loading condition in order to clarify fatigue properties of transverse tracks placed vertically along the welding line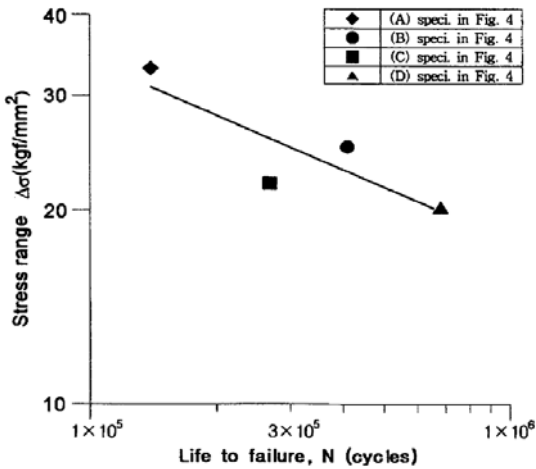 — Fig. 3. Also, fatigue tests were performed on specimens with transverse cracks both on the surface and inside so as to determine fatigue properties depending on crack location.

3. Result and Discussion

The position of transverse cracks was verified by ultrasonic nondestructive examination. The surface of the weld bead was then cut at 0.5-mm-depth intervals using a milling machine and checked for accurate position and length of the transverse crack using ultrasonic testing and magnetic particle inspection after each machining step. Figure 4 shows crack morphology after magnetic particle inspection of specimens with transverse tracks on the surface. Figure 5 shows the results of the fatigue tests of specimens with surface cracks. Maximum load of the fatigue test was in the range of 50% yield strength. The specimen in Fig. 4(a) had a 1.4×10^5 fatigue life when the load was 33 kgf/mm². The crack did not propagate where it was long (a-1), but rather where it was short (a-2). It was revealed by fracture analysis after the fatigue test that a-1 had less than a 1-mm transverse crack depth, while a-2 had a transverse crack depth of 2-3 mm. Specimen b, where the crack grew at b-1 and was coalesced at

Fig. 4   The morphology of surface cracks after magnetic particle inspection of FCAW deposits

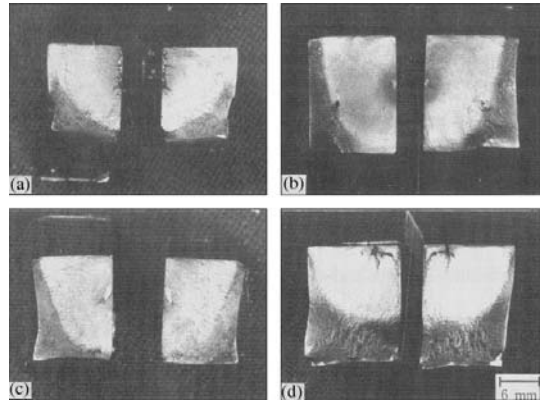**Fig. 6**   Fractures of fatigue-tested specimens with surface cracks

Fig. 5   Fatigue test result of welds with surface cracks

b-2, had 4.1×10^5 fatigue life. Most cracks are multiple surface cracks that easily coalesce and don't grow like single cracks, increasing the possibility of unstable destruction. According to ASME Boiler and Pressure Vessel Code (1995) the definition of coalescence of adjacent surface cracks is as follows :

(1) Discontinuous indications that are coplanar and nonaligned in the through-wall direction of the section thickness, and have at least one indication characterized as a surface check, if the separation distances S1 and S2 between the individual cracks are equal to or less than the dimensions.

(2) The dimensions a and l of the combined single crack of 1 above shall be defined by the size of the bounding square or rectangle that contains the individual nonaligned crack.

(3) Discontinuous indications that are coplanar and nonaligned in the through-wall direction of the section thickness and characterized as surface cracks shall be considered single planar subsurface cracks if the separation distances S1, S1, S3 and S4 are equal to or less than the dimensions.

Specimen c was tested under a load of 22 kgf/mm² and was fractured at c-1 with 4.1×10^5 fatigue life. Specimen c showed shorter fatigue life than specimen b even at low load condition. It seems there was stress concentration at the crack on the specimen edge. Specimen d was fatigue tested under a load of 20 kgf/mm² and was fractured at d-1 with 6.8×10^5 fatigue life. Figure 6 shows fractures after fatigue testing various specimens with surface cracks. Cracks on the surface center propagate like a half ellipse, while cracks on surface edge propagate like a quarter circle.

Figure 7 shows the results from fatigue testing specimens with Internal cracks. It indicates a 2.0×10^6 fatigue limit at design stresses of 25 and 30 kgf/mm² load conditions. This result was quite different from the surface cracks shown in Fig. 5. The internal-crack specimens showed high fatigue strength, while the surface-crack specimen showed low fatigue strength from the stress concentration caused by the notch effect. Therefore, it
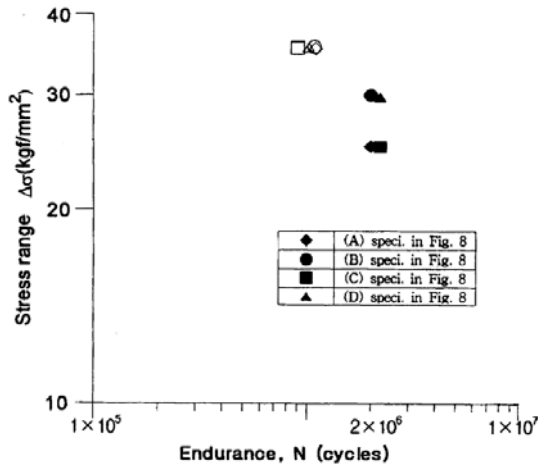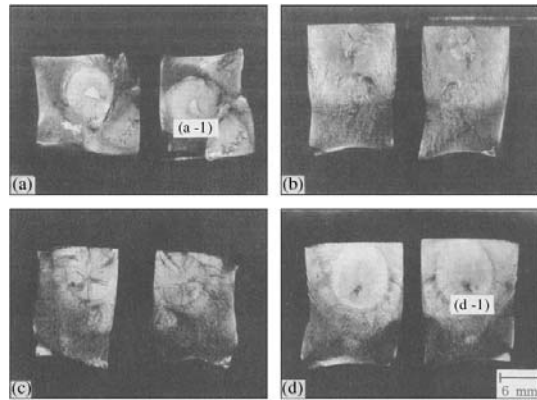
Fig. 7 Fatigue test results of specimens with internal cracks (blank symbols represent life to failure in the range of 35 kgf/mm² load condition)

Fig. 8 Fracture surface of specimens with internal cracks after fatigue testing at 35 kgf/mm² stress range (each specimen was overloaded by 35 kgf/mm²) stress range in order to fracture the specimen artificially

was presumed the internal crack was not much affected by stress concentration. Blank symbols shown in Fig. 7 represent fatigue life to failure in the range of 35 kgf/mm² load condition. Fatigue leading of 35 kgf/mm², which is in the yield stress range of the base metal, was applied in order to fracture the specimen artificially (each specimen was overloaded to 35 kgf/mm² stress after fatigue testing).

Figure 8 shows the fractured surface after fatigue testing (load 35 kgf/mm²) specimens with internal cracks. Propagation showed circular or elliptical morphology. The specimens with surface cracks showed half- or quarter-circle morphology, while the specimen with internal cracks showed circle-shaped morphology. These were somewhat different results compared to the surface cracks shown in Fig. 6.

General crack size and location were checked by ultrasonics before fatigue testing. The internal cracks had 2~5 mm length with some intervals. Transverse cracks less than 2 mm and porosity were located some distance from each other, especially in the case of Fig. 8(d). Figures 8(a), (b) and (c) show the transverse crack was the cause of fracture, while Fig. 8(d) shows porosity was the cause of fracture. This result was also observed by scanning electron microscope — Fig. 9. From this observation, it appears the fatigue

crack does not start at the crack but rather at porosity because the fatigue crack has more cross section than crack area.

Generally, surface cracks propagate more rapidly at a sharp edge than at porosity. But with internal cracks, the cross-section area has the greatest effect on fatigue strength. Robakowski et al. (1987), showed the position and dimension of weld discontinuities greatly affect fatigue strength. Fatigue test samples of high-strength steel, which had 16 mm thickness and 500-MPa (51 kgf/mm²) yield strength, showed a fatigue limit of 140 MPa (14 kgf/mm²) when linear slag inclusion (internal discontinuities) was no longer than 3 mm and less than 10% of specimen cross section.

According to this result, the fatigue strength was relatively lower than that of this study, which had a fatigue limit of 30 kgf/mm² for material having a yield strength 64 kgf/mm².

Hairline-sized transverse cracks showed relatively high fatigue strength because they were smaller than porosity of slag inclusions. In conclusion, if internal discontinuities have a small cross section, as in the transverse cracks of the test samples, fatigue strength isn't much affected.

Figure 9 shows scanning electron microscope (SEM) images around the discontinuities shown in Fig. 8. Figures 9(a), (b) and (c) show the fractured transverse crack area, as indicated in
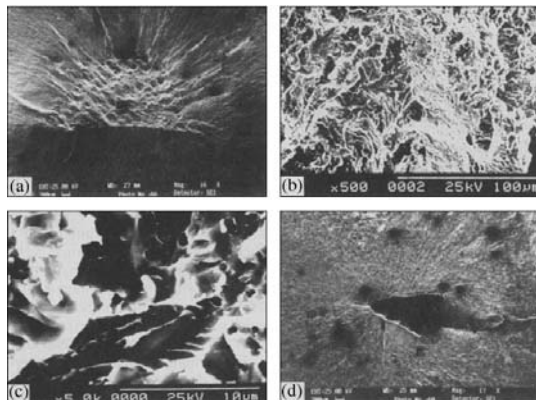
Fig. 9 SEM morphology of cracks and porosity
(a) Crack (16X) (b) Crack (500X)
(c) Crack (5000X) (d) Porosity (17X)

Fig. 8(a), and it consists of quasi- cleavage and microvoid. It is a morphology of a typical cold crack (Lee and Kang, 1997). Figure 9(d) is magnified porosity in Fig. 8(d).

5. Conclusions

Fatigue strength depending on crack position was studied in weld metal deposited using the FCAW process. The results of this study are su mmarized as follows :

(1) Transverse cracks propagate like a quarter of half circle, and specimens with surface cracks broke at low cycle. This was especially true with specimens exhibiting surface edge cracks, which showed relatively low fatigue strength due to stress concentration. Adjacent surface cracks coalesced, speeding fatigue fracture.

(2) Specimens with internal cracks showed superior fatigue strength, enough to reach fatigue limit under designed stress. Propagation mode showed a circular or elliptical morphology.

(3) Specimens with internal cracks and poros-ity showed fatigue fracture at the large cross-sec-tional area of the porosity. Therefore, it appears the cross-sectional area of a discontinuity has

greater effect on fatigue strength than its shape.

References

Boiler and Pressure Vessel Code, Section XI, 1995, American Society of Mechanical Engineers, pp. 20~23.

Dreng, T., Robakowshi and Dreng, and Scierski, J. M., 1987, International Conference on Fatigue of Welded Constructions, England, Welding Institute, pp. 445~456.

Forrnan, R. G., 1972, "Study of Fatigue Crack Initiation from Flaws Using Fracture Mechanics Theory," *Eng. Fract. Mech.*, Vol. 4, pp. 333~345.

Lee, H. W. and Kang, S. W., 1997, "A Study on Transverse weld Cracks in 50- mm Thick Steel Plate with the SAW Process," *Journal of Japan Welding Society*, Vol. 15, No. 4, pp. 563~573.

Lee, H. W., Kang, S. W. and Um, D. S., 1998, "A Study on Transverse weld cRacks in Thick Steel Plate with the FCAW Process," *Welding Journal*, Vol. 77, No. 12, pp. 503~510.

Lu, B., Zheng, X. and Li, D., 1993, "Fatigue Crack Initiation and Propagation in Butt-Joint weld of an Ultrahigh-Strength Steel," *Welding Journal*, Vol. 72, No. 2, pp. 79~86.

Structural Welding Code — Steel (ANSI/AWS D1.1-98), American Welding Society, Miami, Fla., pp. 175~180.

Tsay, L. W., Chen, T. S., Gau, C. Y. and Yang, J. R., 1999, "Microstructure and Fatigue Crack Growth of EH36 TMCP Steel weldments," *International Journal of Fatigue 21*, pp. 857~864.

Yurioka, N., 1995, "A Chart Method to Determine Necessary Preheat Temperature in Steel Welding," *Journal of Japan Welding Society*, pp. 347~350.

Zhang, M., Yang, P. and Tan, Y., 1999, "Micro-mechanisms of Fatigue Crack Nucleation and Short Crack Growth in Low Carbon Steel Under Low Cycle Impact Fatigue Loading," *International Journal of Fatigue 21*, pp. 823~830.